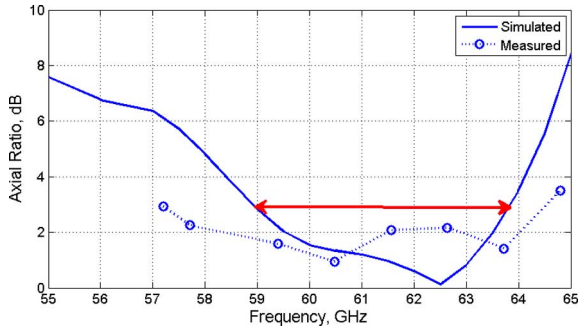

Fig. 8. Simulated and measured antenna-in-package AR over the 60 GHz frequency range.

Simulated results show that the antenna has an AR bandwidth of 5 GHz. Measurements show that the AR bandwidth is close to 7 GHz.

IV. Conclusions

It was shown that the single arm rectangular spiral antenna is a suitable solution for mm-wave short range application. This antenna provides circular polarization with a compact and simple structure. This antenna has a broadband performance with 33% relative bandwidth. The axial ratio bandwidth of this antenna can be as large as 22%. The designed antenna can be easily integrated in a multi-layer package. The antenna structure can be modified to compensate for the packaging effects. The measured results for a 60 GHz implementation of the square spiral antenna in-package show more than 12 GHz of impedance bandwidth, 7 GHz of axial-ratio bandwidth, and 6 dBi gain. The antenna efficiency, calculated at the die pad, ranges from 65% to 75%. Use of this fully planar CP antenna, where feed and antenna located on the same layer, reduces the packaging cost and height significantly.

References

[1] T. Manabe, Y. Miura, and T. Ihara, "Effects of antenna directivity and polarization on indoor multipath propagation characteristics at 60 GHz," *IEEE J. Sel. Areas Commun.*, vol. 14, no. 3, pp. 441–448, 1996.

[2] K.-L. Wong, *Compact and Broadband Microstrip Antennas*, 1st ed. New York, NY, USA: Wiley-Interscience, 2002.

[3] D. Liu, J. A. Akkermans, H.-C. Chen, and B. Floyd, "Packages with integrated 60-GHz aperture-coupled patch antennas," *IEEE Trans. Antennas Propag.*, vol. 59, no. 10, pp. 3607–3616, Oct. 2011.

[4] A. R. Weily and Y. J. Guo, "Circularly polarized ellipse-loaded circular slot array for millimeter-wave WPAN applications," *IEEE Trans. Antennas Propag.*, vol. 7, no. 10, pp. 2862–2870, Oct. 2009.

[5] H. Sun, Y.-X. Guo, and Z. Wang, "60-GHz circularly polarized U-slot patch antenna array on LTCC," *IEEE Trans. Antennas Propag.*, vol. 61, no. 1, pp. 430–435, Jan. 2013.

[6] Y. P. Zhang, M. Sun, K. M. Chua, L. L. Wai, and D. Liu, "Antenna-in-package design for wirebond interconnection to highly integrated 60-GHz radios," *IEEE Trans. Antennas Propag.*, vol. 57, no. 10, pp. 2842–2852, Oct. 2009.

[7] B. Zhang and Y. P. Zhang, "Grid array antennas with subarrays and multiple feeds for 60-GHz radios," *IEEE Trans. Antennas Propag.*, vol. 60, no. 5, pp. 2270–2275, May 2012.

[8] C. Liu, Y.-X. Guo, X. Bao, and S.-Q. Xiao, "60-GHz LTCC integrated circularly polarized helical antenna array," *IEEE Trans. Antennas Propag.*, vol. 60, no. 3, pp. 1329–1335, Mar. 2012.

[9] R. Zhou, D. Liu, and H. Xin, "Design of circularly polarized antenna for 60 GHz wireless communications," in *Proc. EuCAP*, 2009, pp. 3787–3789.

[10] H. Nakano, J. Eto, Y. Okabe, and J. Yamauchi, "Tilted- and axial-beam formation by a single-arm rectangular spiral antenna with compact dielectric substrate and conducting plane," *IEEE Trans. Antennas Propag.*, vol. 50, no. 1, pp. 17–23, Jan. 2002.

[11] J. T. Bernhard, "Compact single-arm square spiral microstrip antenna with tuning arms," in *Proc. IEEE Int. Antennas Propagation Symp.*, Jul. 8–13, 2001, vol. 2, pp. 696–699.

[12] M. Fakharzadeh *et al.*, "CMOS phased array transceiver technology for 60 GHz wireless applications," *IEEE Trans. Antennas Propag.*, vol. 58, no. 4, pp. 1093–1104, Apr. 2010.

[13] M. Fakharzadeh and L. Verma, "PHY front end design for emerging 60 GHz multi-gigabit wireless devices," in *Proc. 10th IEEE CCNC*, Las Vegas, NV, USA, Jan. 2013, pp. 817–820.

[14] L. Verma, M. Fakharzadeh, and S. Choi, "Wi-Fi on steroids: 802.11ac and 802.11ad," *IEEE Wireless Commun. Mag.*, vol. 20, no. 6, pp. 30–35, Dec. 2013.

[15] R. A. Alhalabi, Y. C. Chiou, and G. M. Rebeiz, "Self-shielded high-efficiency Yagi-Uda antennas for 60 GHz communications," *IEEE Trans. Antennas Propag.*, vol. 59, no. 3, pp. 742–750, Mar. 2011.

Compact Antenna With U-Shaped Open-End Slot Structure for Multi-Band Handset Applications

Cho-Kang Hsu and Shyh-Jong Chung

***Abstract*—This communication proposes a compact U-shaped slot antenna with a coupling feed for 4G handset applications. The antenna is composed of a simple open-end U-shaped slot and a feeding line with an antenna area of 58 mm × 12 mm. Two types of resonant modes are excited, including slot mode and monopole mode. Parametric studies on the slot geometry have been demonstrated. By controlling the related parameters, the bandwidth of this antenna can potentially cover the mobile bands of LTE Band 12 (698–742 MHz)/DCS (1710–1880 MHz)/PCS (1850–1990 MHz)/UMTS (1920–2170 MHz)/LTE Band 40 (2300–2400 MHz)/Band 41 (2496–2690 MHz)/Band 42 (3400–3600 MHz)/Band 43 (3600–3800 MHz). Good radiation characteristics, like gain and radiation efficiency are obtained over these operating bands. This antenna is suitable for the metal casing of handheld devices.**

***Index Terms*—Cellular phone antennas, mobile phone antennas, multi-band antenna, slot antenna.**

I. Introduction

With the growing demand for communication systems, antennas on handheld devices are needed to support multiple bands of 2G, 3G and 4G. Handheld devices are preferred to be light-weight, thin, and fashionable, and as a result, metal casings have become popular. However, the bandwidth and radiation efficiency of conventional antennas in handheld devices tend to decrease when antenna in proximity of metal casings. Examples include the monopole and inverted-F antennas. Therefore, slot antennas become attractive for handheld devices with metal casings.

Various slot antenna structures, including circular [1], triangles [2] and fractal shape [3], have been proposed to achieve a wide impedance bandwidth. A wide slot might support numerous resonance modes, and two nearby resonance modes can be merged to form a wider bandwidth [4]. However, because these designs require a large area for slot, they are not suitable for handheld devices.

To reduce the overall size of a multi-band slot antenna, various designs have been produced. Some quarter-wavelength open slots are designed in [5] and [6] to achieve a compact size. In [7] and [8], multiple bandwidths are achieved with several independent slots that operate

Manuscript received May 28, 2013; revised August 19, 2013; accepted October 24, 2013. Date of publication November 07, 2013; date of current version January 30, 2014.

The authors are with the Department of Communication Engineering, National Chiao-Tung University, Hsinchu 300, Taiwan, ROC (e-mail: drokun.tw@gmail.com; sjchung@cm.nctu.edu.tw).

Digital Object Identifier 10.1109/TAP.2013.2289996

0018-926X © 2013 IEEE. Personal use is permitted, but republication/redistribution requires IEEE permission.
See http://www.ieee.org/publications_standards/publications/rights/index.html for more information.

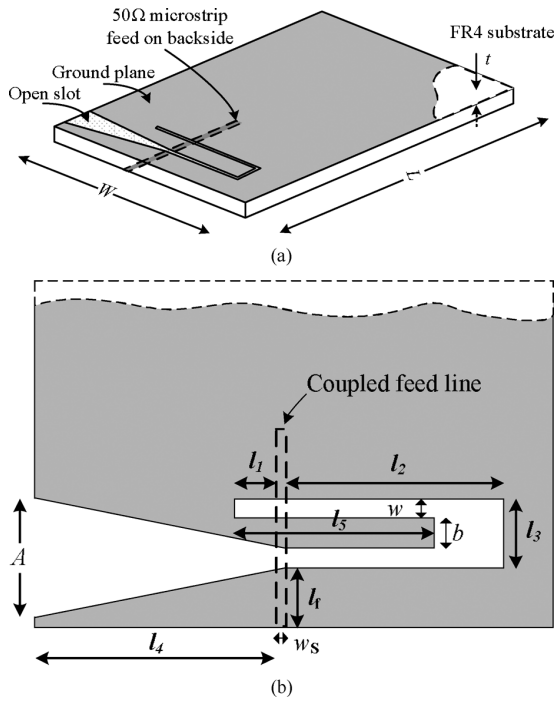

Fig. 1. (a) Configuration of the proposed antenna, (b) detail dimensions.

using half-wavelength mode. A combination of a planar inverted-F antenna (PIFA) and a slot in the ground plane was used to achieve a small footprint and low profile in [9]–[11]. Multi-strip monopole antenna and slotted ground plane (the slots add additional resonant modes) can be merged to form an antenna with a wider bandwidth [12]–[14]. In [15], a tunable dual-band slot antenna was designed by varying the capacitance of a varactor across the slot.

With the above miniaturization and bandwidth enhancement methods, the operation bands of the slot antennas increased from a single band to multiple bands. However, achieving multi band slot antennas within a compact structure is still a challenge. This study proposes a compact multi-band antenna composed with a straight coupled-fed microstrip line, a U-shaped slot, and a tapered open-end to generate four resonance modes, including two slot modes and two monopole modes. The advantage of proposed structure is to obtain wide bandwidth (1700–4200 MHz) on the high frequency to cover more bands. This result is better than the bandwidth of reference papers [5]–[15] (1700–2800 MHz). The details of the operating principle, the design procedure, and the measured and simulated results are presented and discussed. All the simulations in this study are performed using an Ansoft high-frequency structure simulator (HFSS) based on the finite element method that is used for full-wave 3D EM simulation, which helps benefic to obtain the required antenna dimensions and performance.

II. Antenna Design

A. Antenna Configuration

Fig. 1 shows the configuration of the U-shaped open-end slot antenna, which was fabricated on an FR4 substrate ($\varepsilon_r = 4.43$) with a thickness $\mathrm{t} = 0.6\ \mathrm{mm}$ and 65 mm × 120 mm with copper on one side. The proposed structure can be viewed as a rectangular aperture of size $(l_1 + w_\mathrm{s} + l_2) \times l_3$, in which a metal strip of dimension $l_5 \times b$ was inserted, leaving a slot of width w on the upper and lower edges of the aperture, to construct a U-shaped slot. At one end of the U-shaped slot, a tapered open-end structure was connected. A 50 ohm microstrip line of width $w_\mathrm{s} = 1.1\ \mathrm{mm}$ was printed on the opposite side of the ground plane to form a coupled feed.

B. Resonance Mechanisms

The design of the U-shaped open-end slot antenna was simple and could be clearly understood. The path of the open-end slot of $l_1 + 2 \times l_2 + l_3 + l_4$, also called a monopole slot [5], provided the longest resonant path to generate a quarter-wavelength mode at low frequency. Two strips, l_4, l_5, were excited using the coupled feed line. The open end microstrip line of length l_f and $l_\mathrm{f} + l_3/2$ provide the effective coupling capacitances to produce the energy coupling on the l_4 and l_5, respectively, to generate two quarter-wavelength monopole modes at high frequency. In addition, the area between the U-shaped slot of length $2 \times l_2 + l_3$ and the microstrip line l_3 truncated by the slot lines formed a rectangular looped path to generate one wavelength slot resonance on high frequency. Four resonant modes were excited using the proposed structure. The relative calculation of resonant frequency for the four modes is listed as follows

$$f_{r1} \cong \frac{c}{4 \cdot \left(l_1 + 2 \cdot l_2 + l_3 + \frac{2}{3} l_4\right)} \tag{1}$$

$$f_{r2} \cong \frac{c}{4 \cdot \tau \cdot l_5} \tag{2}$$

$$f_{r3} \cong \frac{c}{4 \cdot l_4} \tag{3}$$

$$f_{r4} \cong \frac{c}{2 \cdot (l_2 + l_3)}. \tag{4}$$

The current distributions of the proposed structure were observed to further explain their resonant behavior. Fig. 2(a) shows the current distribution on the monopole slot mode. This path resonated at 720 MHz. Note that the wider the tapered open-end slot is, the shorter the effective slot length is. In our simulation, it is found that most of the induced current concentrates around the tapered slot of a $2/3 \times l_4$ length. Fig. 2(b) shows the current distribution in the right strip, which has dimensions of $l_5 \times b$. This path resonated at 1.76 GHz, like a monopole antenna in its fundamental mode. The strip was closely surrounded by the ground, incurring a strong capacitive effect, thus reducing its resonant frequency and bandwidth. The correlative parameter τ in (2) was approximately 1.36 in value. Fig. 2(c) shows the current distribution on the left strip, which had approximate dimensions of $l_4 \times l_\mathrm{f}/2$. This path resonated at 2.4 GHz, which was also similar to a monopole antenna at the fundamental mode. The purpose of the taper open-end structure was applied to excite the wider impedance bandwidth of the monopole mode on l_4 because the ground was distant. Fig. 2(d) shows the current distribution in the area between the U-shaped slot and the microstrip line truncated by the slot lines. The microstrip feed line provided two virtual shorts to form a path that resonates at 3.5 GHz. It was associated with the current flows around the U-shaped slot that generate one wavelength slot mode.

C. Antenna Parametric Study

The performance of the proposed antenna was related to the antenna geometry. A length of l_f provided the reactive loading. It mainly affected the impedance matching of the antenna's lower and upper bands [16]. By tuning various parts, different modes could be adjusted to resonate at desired frequencies. The variation of the pivotal geometrical parameters l_2, l_4, l_5, and A in the resonant frequencies was studied. Each pivotal parameter was varied while the others were not changed.

Fig. 3 shows that as l_5 decreased from 31 to 25 mm, the fundamental resonant frequencies of the strip-monopole increased from 1.74 to 2.09 GHz. In addition, as l_5 decreased, the separation between the strip and the surrounding ground increased, leading to a wider radiating aperture area for a slot mode at 3.5 GHz. The impedance bandwidth of this slot mode increased slightly.

Fig. 4 shows the effect of l_4 on the resonant frequencies. The fundamental mode of the strip-monopole was affected by l_4. When l_4 decreased from 30 to 21 mm, the resonant frequency increased from

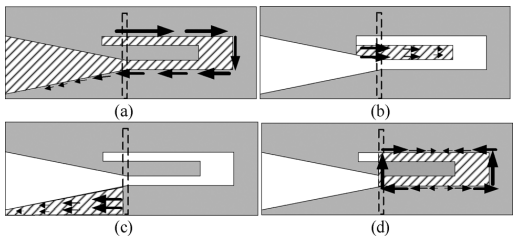

Fig. 2. Typical current distribution of (a) the first resonant mode at 720 MHz, (b) the second resonant mode at 1.76 GHz, (c) the third resonant mode at 2.4 GHz, and (d) the fourth resonant mode at 3.5 GHz.

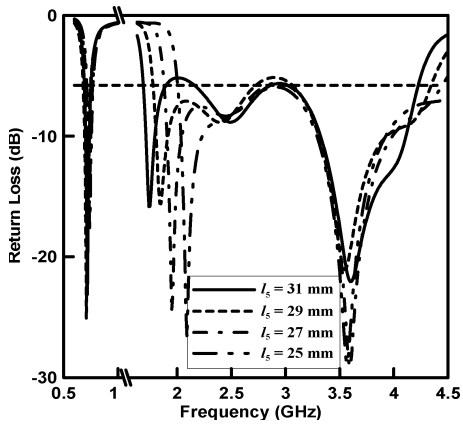

Fig. 3. Simulated S11 for several values of l_5.

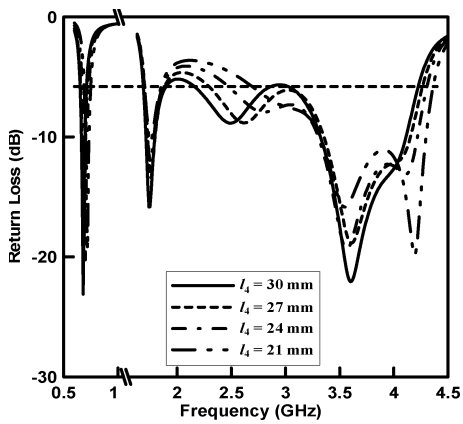

Fig. 4. Simulated S11 for several values of l_4.

2.4 to 3.1 GHz. An extra resonance, which appears at 4.2 GHz, is a higher-order mode that resonated at the half wavelength along the l_4 strip. In addition, as l_4 decreased, the resonant frequency at 0.72 GHz was rarely affected because the weak current distribution of open-end slot mode was at the end of the tapered structure.

When the aperture length l_2 decreased from 33 to 30 mm, the resonant frequency of the slot mode increased from 3.4 to 3.8 GHz, as shown in Fig. 5. In addition, the aperture length l_2 also affected the open-end slot mode. As length of the slot decreased, the resonant frequency increased from 0.72 to 0.8 GHz.

The taper aperture dimension A at the end of the open-end slot affected the monopole mode and the open-end slot mode. Fig. 6 shows the effect of A on the resonant frequencies. When the A decreased from 11 to 2.5 mm, the separation between the l_4 strip and the ground was reduced, leading to the poor impedance matching of the monopole mode, which resonated at 2.4 GHz. On the other hand, the reduced A extended the physical length of the open-end slot. The resonant frequency of the open-end slot mode decreased from 0.72 to 0.65 GHz.

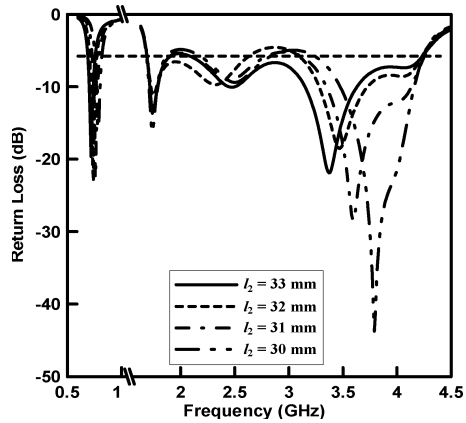

Fig. 5. Simulated S11 for several values of l_2.

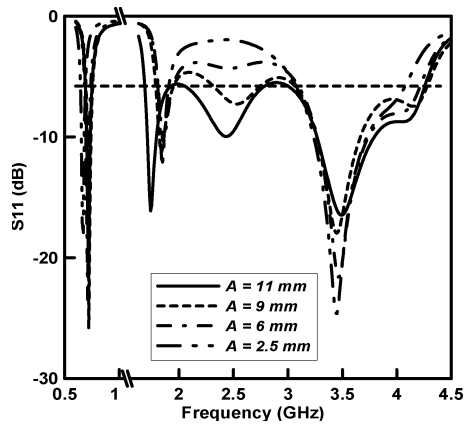

Fig. 6. Simulated S11 for several values of A.

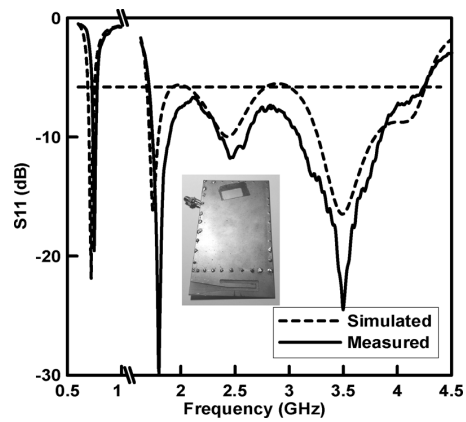

Fig. 7. Measured and simulated S11 of proposed U-shaped open-end slot antenna. Shown in the inset is the photo of the fabricated prototype.

III. Experimental Results

Based on the optimized design dimensions shown in Table I, the prototype of the proposed antenna was constructed and tested. Fig. 7 shows the measured and simulated S11, shown in the inset is the photo of the fabricated prototype. The agreement between measurement and simulation can be seen. The experimental tolerance originated from the test cable that connected the antenna to the measurement equipment [17]. The measured data shows that several resonant modes were successfully excited, and the antenna shows an extremely wide impedance bandwidth on the high frequency. With an impedance bandwidth of VSWR $<$ 3, which is commonly used for mobile phone antenna designs, the lower band had a bandwidth of approximately 60 MHz, ranging from 690 MHz to 750 MHz and covering the LTE700 operation. Regarding the upper band, considerably larger bandwidth formed by three resonances was obtained. The bandwidth approaches 2500

TABLE I
PRINCIPAL DIMENSIONS OF THE PROPOSED ANTENNA

Dimension	Length (mm)	Dimension	Length (mm)
l_1	2	w	2.5
l_2	33	w_S	1.1
l_3	7	b	2
l_4	30	W	65
l_5	31	L	120
A	10	t	0.6
l_f	5		

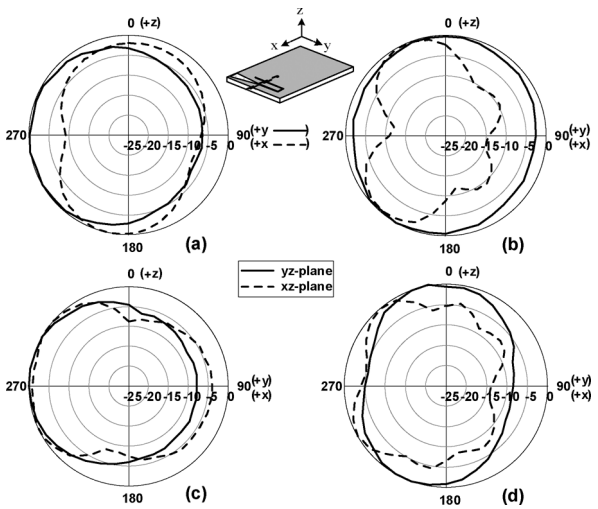

Fig. 8. Measured normalized total radiation field patterns of total power at (a) 690, (b) 1760, (c) 2400 and (d) 3500 MHz for the fabricated prototype in the xz-plane and yz-plane. (Unit: dBi).

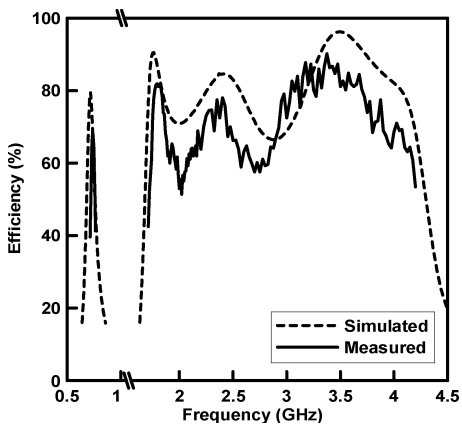

Fig. 9. Simulated and measured total radiated efficiency of the proposed antenna.

MHz, ranging from 1700 MHz to 4200 MHz and nearly covers the entire requirement of the phone system for high frequency, such as DCS, PCS, UMTS, EVDO, LTE, TD-LTE and WiMAX.

The total radiation field patterns and the total radiated efficiency were measured in a 3D anechoic chamber. Fig. 8(a)–(d) show the measured normalized total radiation field patterns at 690 MHz, 1760 MHz, 2400 MHz and 3500 MHz, respectively, in the xz- and yz-planes. The radiation patterns were basically omni-directional, with minor nulls in certain directions. The peak gain was approximately 0.8 dBi at 690 MHz. In the high-frequency rang e, the peak gain varied from 0.6 dBi to 2.1 dBi. Regarding the practical application, the total radiated efficiency could be an important parameter to describe the antenna performance. The simulated and measured total radiated efficiency were analyzed, as shown in Fig. 9. In the low frequency, the total radiated efficiency exceeded 58%. In the high frequency, the widely continuous total radiated efficiency that was obtained exceeded 50%. The results can be appropriately applied to mobile phones.

IV. CONCLUSION

This communication proposed a wide-band U-shaped open-end slot antenna for handheld devices. Complete analyses of its geometrical parameters were studied. Its impedance bandwidth covered the frequencies of 690 to 750 MHz and 1700 to 4200 MHz, enabling it for mobile phone system application. Detailed design considerations for the antenna were described. Four operating resonant modes were identified, and the effects of different parameters on these modes were analyzed. The radiation efficiency was also presented and appropriate radiation characteristics were obtained.

REFERENCES

[1] S. W. Qu, J. L. Li, J. X. Chen, and Q. Xue, "Ultrawideband strip-loaded circular slot antenna with improved radiation patterns," *IEEE Trans. Antennas Propag.*, vol. 55, no. 11, pp. 3348–3353, Nov. 2007.

[2] W. S. Chen and F. M. Hsieh, "Broadband design of the printed triangular slot antenna," in *Proc. IEEE APS Int. Symp.*, Jul. 2004, vol. 4, pp. 3733–3736.

[3] W. L. Chen, G. M. Wang, and C. X. Zhang, "Bandwidth enhancement of a microstrip-line-fed printed wide-slot antenna with a fractal-shaped slot," *IEEE Trans. Antennas Propag.*, vol. 57, no. 7, pp. 2176–2179, Jul. 2009.

[4] J. Y. Jan and J. W. Su, "Bandwidth enhancement of a printed wide-slot antenna with a rotated slot," *IEEE Trans. Antenna Propag.*, vol. 53, no. 6, pp. 2111–2114, Jun. 2005.

[5] C. I. Lin and K. L. Wong, "Printed monopole slot antenna for internal multiband mobile phone antenna," *IEEE Trans. Antennas Propag.*, vol. 55, no. 12, pp. 3690–3697, Dec. 2007.

[6] Y. Cao, B. Yuan, and G. Wang, "A compact multiband open-ended slot antenna for mobile handsets," *IEEE Antennas Wireless Propag. Lett.*, vol. 10, pp. 911–914, 2011.

[7] S. H. Lee, Y. Lim, Y. J. Yoon, C. B. Hong, and H. I. Kim, "Multiband folded slot antenna with reduced hand effect for handsets," *IEEE Antennas Wireless Propag. Lett.*, vol. 9, pp. 674–677, 2010.

[8] B. Yuan, Y. Cao, and G. Wang, "A miniaturized printed slot antenna for six-band operation of mobile handsets," *IEEE Antennas Wireless Propag. Lett.*, vol. 10, pp. 854–857, 2011.

[9] A. Cabedo, J. Anguera, C. Picher, M. Ribo, and C. Puente, "Multiband handset antenna combining a PIFA, slots, and ground plane modes," *IEEE Trans. Antenna Propag.*, vol. 57, no. 9, pp. 2526–2533, Sep. 2009.

[10] J. Anguera, I. Sanz, J. Mumbru, and C. Puente, "Multiband handset antenna with a parallel excitation of PIFA and slot radiators," *IEEE Trans. Antenna Propag.*, vol. 58, no. 2, pp. 348–356, Feb. 2010.

[11] R. Hossa, A. Byndas, and M. E. Bialkowski, "Improvement of compact terminal antenna performance by incorporating open-end slots in ground plane," *IEEE Microwave Wireless Compon. Lett.*, vol. 14, no. 6, p. 283, Jun. 2004.

[12] C. L. Liu, Y. F. Lin, C. M. Liang, S. C. Pan, and H. M. Chen, "Miniature Internal Penta-band monopole antenna for mobile phones," *IEEE Trans. Antennas Propag.*, vol. 58, no. 3, Mar. 2010.

[13] G. Kang, Z. Du, and K. Gong, "Compact broadband printed slot-monopole-hybrid diversity antenna for mobile terminals," *IEEE Antennas Wireless Propag. Lett.*, vol. 10, pp. 159–162, 2011.

[14] A. Boldaji and M. E. Bialkowski, "A compact hepta-band antenna for portable and embedded devices," *Microwave Opt. Technol. Lett.*, vol. 54, no. 7, pp. 1614–1618, Jul. 2012.

[15] N. Behdad and K. Sarabandi, "A varactor-tuned dual-band slot antenna," *IEEE Trans. Antenna Propag.*, vol. 54, no. 2, pp. 401–408, Feb. 2006.

[16] Y. S. Wang and S. J. Chung, "A short open-end slot antenna with equivalent circuit analysis," *IEEE Trans. Antennas Propag.*, vol. 58, no. 5, pp. 1771–1775, Mar. 2010.

[17] Z. N. Chen, N. Yang, Y. X. Guo, and Y. W. Chia, "An investigation into measurement of handset antennas," *IEEE Trans. Instrum. Meas.*, vol. 54, no. 3, pp. 1100–1110, Jun. 2005.